ENVIRONMENTAL RESEARCH
LETTERS

Temporal changes in the Euphrates and Tigris discharges and teleconnections

To cite this article: O L Sen *et al* 2011 *Environ. Res. Lett.* **6** 024012

Environ. Res. Lett. **6** (2011) 024012 (9pp) doi:10.1088/1748-9326/6/2/024012

Temporal changes in the Euphrates and Tigris discharges and teleconnections

O L Sen[1], **A Unal, D Bozkurt and T Kindap**

Istanbul Technical University, Eurasia Institute of Earth Sciences, Maslak 34469, Istanbul, Turkey

E-mail: senomer@itu.edu.tr

Received 24 October 2010
Accepted for publication 13 May 2011
Published 26 May 2011
Online at stacks.iop.org/ERL/6/024012

Abstract
The streamflow timings of the Euphrates and Tigris, two important snow-fed rivers in the Middle East, are found to be shifting to earlier days in the year. Six out of eight stations indicate statistically significant shifts between two consecutive 17-year periods (i.e. 1972–88 and 1990–2006). Among these stations, the average shift to earlier times is over 5 days, suggesting earlier spring melting of snowpack due to increased temperatures in the second period. A striking increase in the discharges takes place during the first half of March, and it is observed at all stream gauging sites considered in this study. An analysis based on the NCEP/NCAR reanalysis data indicates that warming which results in this increase is associated with the switching from the northeasterly flow to southwesterly flow over the Black Sea and western Anatolia caused by the weakening of the Siberian High over eastern Europe. These changes in the circulation features from the first to second periods are found to be very consistent with the positive and negative phases of the North Sea–Caspian pattern.

Keywords: Turkey, hydroclimatology, streamflow, center time, NCP

1. Introduction

Temperature has been traditionally used as the primary parameter in detecting climate change signals at scales from local to global. As point measurements, however, temperature data come with important shortcomings such as inadequate representation of mountainous areas and contamination by urban heat island effects as most stations are located in cities (e.g. Ezber *et al* 2007). Given the sensitivity of snowmelt to temperature, the snow-fed river discharge data provide an opportunity to explore the climate change signal over large areas that are relatively free of human influence. In recent years, several studies have been carried out utilizing primarily snow cover and snowmelt derived runoff data to assess the climate change signal in different parts of the world including the North American mountain ranges (e.g. Cayan *et al* 2001, McCabe and Clark 2005, Stewart *et al* 2005, Hamlet *et al* 2007), the Tibetan Plateau and Himalayas (e.g. Zhao and Moore 2006), the Alps in Europe (e.g. Vincent *et al* 2007), and Northern Eurasia (e.g. Yang *et al* 2007).

Stewart (2009), in his comprehensive review study, suggested that in recent decades snowmelt and snowmelt runoff have generally shifted to earlier times in the Northern Hemisphere. Many of the shifts are large and significant. Cayan *et al* (2001) reported that in the western US, the spring onsets take place earlier (about 5–10 days) after the 1970s. Hodgkins *et al* (2003) showed that after the 1960s, winter/spring center of volume dates occur significantly earlier (about 1–2 weeks) at several stream gauging stations in the northern and mountainous areas of the New England. Stewart *et al* (2005) reported regionally coherent shifts (1–4 weeks) in the timing of the streamflow across most of western North America. There are, however, other studies that report the changes in the snowmelt runoff timing that are small and statistically insignificant (e.g. Moore *et al* 2007).

Any seasonal shifts in snowmelt time will have the potential to create significant ecological as well as socio-economic impacts, ranging from reduced energy production to adverse impacts on ecosystems due to summer droughts. For example, Barnett *et al* (2005) showed that, by 2050 or earlier, less winter snowfall and earlier melting will force

[1] Author to whom any correspondence should be addressed.

the Columbia River system management to make a choice to release water for hydroelectric power in summer and autumn or release water for salmon runs in spring and summer. Payne *et al* (2004) also suggest that the Colombia River system could not provide water for both activities.

The headwaters of two major snow-fed rivers in the Middle East, the Euphrates and Tigris, are in eastern Anatolia. Their basins cover an area of approximately 766 000 km^2 in five countries (i.e. Turkey, Iraq, Syria, Iran, and Kuwait). The Euphrates (with an annual total flow around 30 billion cubic meters) and Tigris (with an annual total flow around 50 billion cubic meters) are the main reasons for the region historically being identified as the 'fertile crescent'. However, with population explosion (i.e. the population in this region quadrupled in 55 years, increased from 46 million in 1950 to 180 million in 2005 (USCB 2009)), these rivers are now at the center of international disputes over water use and availability (Daoudy 2004). The future climate simulations (IPCC 2007) show that the Mediterranean region is one of the most vulnerable zones in the world. Analyzing an ensemble of 12 climate model projections based on the SRESA1B emission scenario (foreseeing a CO_2 concentration of about 720 ppm at the end of the present century and warming projections of 1.7–4.4 °C for the end of the present century (IPCC 2007)), Milly *et al* (2005) report 10–30% reductions in runoff in the Middle East by the year 2050. Thus, a changing climate in the region has the potential to exacerbate water disputes by causing temporal shifts in peak flows as well as reducing total flow (Kundzewicz *et al* 2007).

The objective of the present study is, therefore, to investigate the changes in the discharges of the Euphrates and Tigris rivers for the 35-year period between 1972 and 2006. An attempt is also made to identify the atmospheric changes behind a striking increase in the discharges during the first half of March.

2. Approach

2.1. Data

Streamflow records were obtained from the Turkish General Directorate of Electrical Power Resources Survey and Development Administration Hydro-Climatic Data Network for 21 stations. It should be noted that these two rivers are an essential part of the Southeastern Anatolian Project, a 30-billion-dollar investment which aims to produce energy (SAPRDA 2009) and to irrigate vast semi-arid plains in the southeastern parts of Turkey via constructing 19 hydro-power plants and 22 dams. Streamflow measurements at downstream locations of dams and/or hydro-power plants were excluded in this study since such man-made structures might divert streamflow from its natural characteristics. After filtering the data for location, length, and quality, eight gauging stations remain to be used for analysis. All these stations have 35-year continuous daily measurements between 1972 and 2006. We also used daily surface temperature data in the analysis that were obtained from the Turkish State Meteorological Service for six sites in (or near) the basins that feed the tributaries of the Euphrates and Tigris rivers. Locations of the climate stations as well as streamflow measurement sites are given in figure 1. In order to investigate the corresponding changes in the atmospheric fields, we used data from the NCEP/NCAR reanalysis (Kalnay *et al* 1996).

2.2. Methodology

In order to detect the changes in the streamflow timing, researchers have used different measures, such as 'spring pulse onset' that define the date when snowmelt streamflow begins to cause an increase in discharge in spring or early summer (Cayan *et al* 2001), and 'center time' (CT) that defines the date that marks the timing of the center of mass of annual flow (Stewart *et al* 2005). In this study, we adopted CT as the measure to detect any shifts in streamflow timing. Spring pulse onset dates for the stations were also estimated with the methodology suggested by Cayan *et al* (2001). However, the time series of spring pulse onset were quite noisy compared to those of the CTs (the station average coefficient of variation is found to be 0.09; it is 0.06 in CT). As given by Stewart *et al* (2005), we also recognized that the spring pulse onset methodology is quite sensitive to the early (winter) snowmelt–rainfall runoff peaks, and therefore, it may give false onset dates. Thus, the results of this methodology are not included in this paper.

In the first part of the analysis, we estimated the CT dates and assessed the significance of the differences between two periods using the Monte Carlo test. The CT dates were estimated from the daily streamflow measurements for every year at all measurement sites. The CT data were then divided into two periods of 17 years (i.e. 1972–88 and 1990–2006), and mean values were compared for possible changes (named as actual difference). For this purpose, the Monte Carlo test was utilized, where actual differences in average values are compared with the difference of the averages of the randomly sampled 17 data points from the database. If the actual difference is ranked at 90% or higher probability of the randomly sampled database, then the actual difference is identified to be statistically significant. It should be pointed out that CT data for 1989 (a relatively dry water year (Cullen and deMenocal 2000) with a relatively warm spring) were left out because they were determined to be outliers for all stations (CT values for this year ranged between 2.6–5.2 times the standard deviation lower than the average CTs for the stations). In addition to CT methodology, which provides a time-integrated view of the changes in the streamflow, we illustrate daily as well as monthly differences in the streamflow averages between two periods to show when the changes actually occur. In the second part of the analysis, we used the NCEP/NCAR reanalysis data (surface temperature, 10 m wind fields, 850 hPa level temperature, and 500 hPa level temperature and wind fields) to investigate the changes in the large-scale surface and atmospheric fields that may be related to the striking increase in the discharges at the beginning of the major spring pulse in the second period. To our knowledge, such an event has not been reported in the studies of temporal discharge changes. It is also important to learn more about this event as it may affect the management of several dams on the Euphrates and Tigris rivers.

Figure 1. Topography and rivers of eastern Anatolia (GTOPO30, Global 30 Arc-Second Elevation Data Set, http://eros.usgs.gov/#/Find_Data/Products_and_Data_Available/gtopo30). Also shown are the locations of the streamflow gauging (black full triangles) and climate stations (red full circles) analyzed in this study.

Table 1. Information about the streamflow gauging stations used in this study. (Note: E: Euphrates and T: Tigris.)

Station no.[a]	Name	Latitude	Longitude	Altitude (basin average) [highest elevation] (m)	Drainage area (km^2)	Mean annual flow (m^3 s^{-1})[b]	Median annual flow (m^3 s^{-1})[b]	Fraction of MAMJ[c] discharge (%)	Center time date
2102	E.-Palu	38°41′18″	39°55′52″	852 (1856) [4032]	25 515	242.75	230.11	77	18 April
2122	E.-Tutak	39°32′19″	42°46′49″	1552 (2142) [3505]	5 882	48.24	47.35	79	26 April
2133	E.-Melekbahce	39°02′45″	39°31′34″	875 (1861) [3338]	3 284	85.72	87.73	64	28 April
2156	E.-Bagistas	39°26′05″	38°27′04″	865 (1937) [3530]	15 562	148.95	150.16	58	26 April
2157	E.-Karakopru	38°47′02″	41°29′43″	1250 (1636) [2919]	2 173	25.14	23.17	77	08 April
2164	E.-Cayagzi	38°48′31″	40°33′17″	990 (1753) [2824]	2 232	33.43	31.75	79	11 April
2610	T.-Baykan	38°09′41″	41°46′57″	910 (1620) [2601]	640	18.22	17.48	70	08 April
2620	T.-Uzumcu	37°29′11″	43°33′56″	1072 (2420) [3894]	5 270	58.80	58.35	72	08 May

[a] Station number used in General Directorate of Electrical Power Resources Survey and Development Administration in Turkey.
[b] Mean and median monthly flows and center time dates are calculated for the period 1972–2006.
[c] MAMJ stands for March, April, May, and June.

3. Analyses and results

There are differences in the characteristics of the streamflow gauging stations used in this study, as summarized in table 1. The Palu station, located on the Euphrates, has a drainage area of 25 515 km^2 while the Baykan station, on the Tigris, has a drainage area of 640 km^2. It should be noted that the drainage areas of the three stations (Tutak, Karakopru, and Cayagzi) are actually sub-basins of the basin that feeds the Palu. The average elevations of the basins range from 1620 m (Baykan) to 2420 m (Uzumcu). The Palu station has the highest annual mean and median flows (242.75 m^3 s^{-1} and 230.11 m^3 s^{-1} respectively) while the Baykan has the lowest (18.22 m^3 s^{-1} and 17.48 m^3 s^{-1} respectively). The fractions of March, April, May, and June (MAMJ) discharges range from 58% (Bagistas) to 79% (Tutak and Cayagzi). This is a good indicator of the fact that these rivers are primarily fed by snowmelt runoff. Table 1 also provides the average CT dates for the stations. The Karakopru and Baykan have the earliest CT date (both 8 April) while the Uzumcu has the latest (8 May). The differences in the CT dates occur primarily due to the elevational differences between the basins. At high-altitude basins, such as that of the Uzumcu, lower temperatures slow down the snowmelt process.

As a first step in the analysis, we tested the significance of the changes in the annual flows using the same methodology

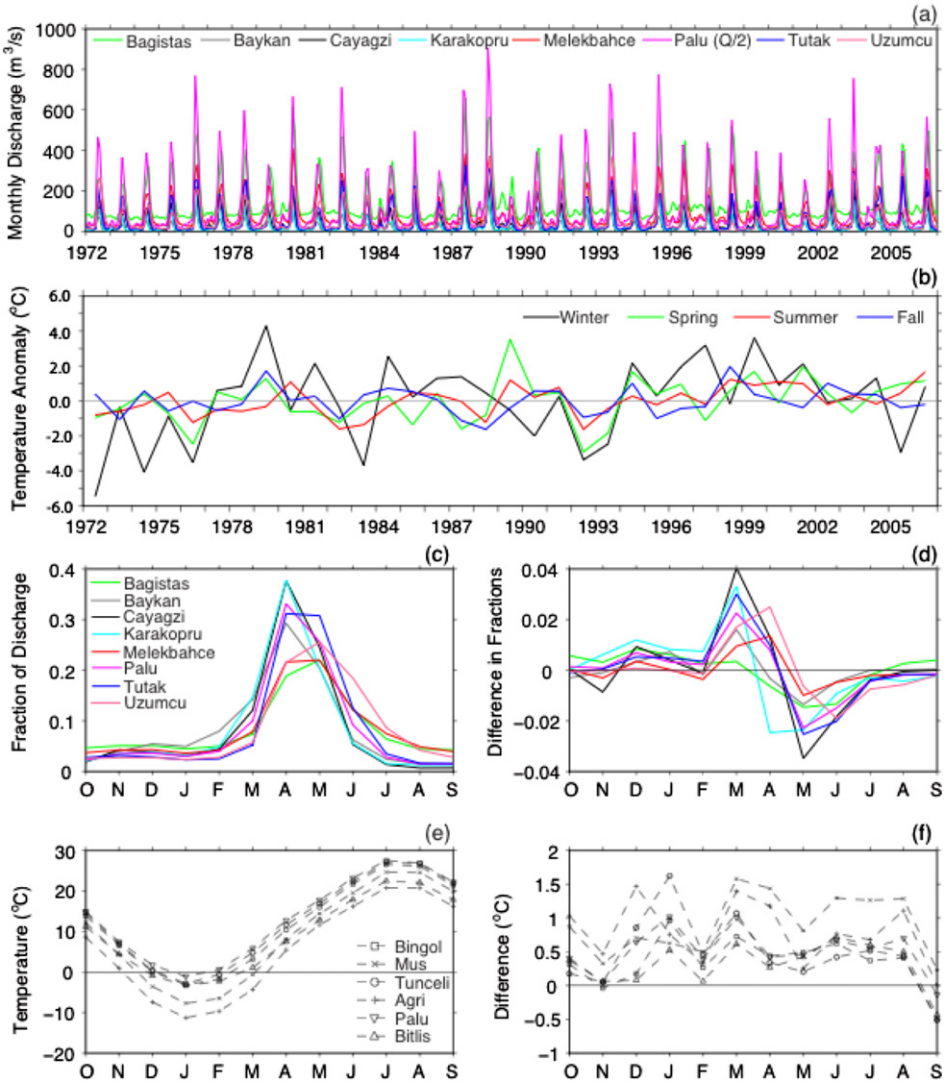

Figure 2. (a) Time series of monthly discharges ($m^3\ s^{-1}$) from the eight stations (halves shown for Palu), (b) time series of seasonal surface temperature anomalies (average for all stations, in °C), (c) monthly streamflow fractions (monthly streamflow over annual streamflow) for the first period (1972–88), (d) changes in the monthly streamflow fractions in the second period (i.e. (1990–2006) minus (1972–88)), (e) monthly surface temperatures (°C) for the first period, and (f) changes in monthly surface temperatures (°C) in the second period.

applied to the CT data. As can be seen in table 2, differences between the two periods (1972–88 and 1990–2006) are not significant at a significance level of 0.1, which suggests that there are no statistically significant changes in the annual flow data. The differences in the CTs of both periods are also provided in table 2 along with the significance test results. Except for the Baykan and Melekbahce, differences in the CTs are found to be statistically significant at a significance level of 0.1. Among significant sites, the average shift in the CT is 5.2 days. The longest shifts are calculated for the Karakopru on the Euphrates and the Uzumcu on the Tigris (both 6.8 days). The 4.8-day shift in the Palu whose drainage area is the largest amongst the stations is also statistically significant.

Monthly discharges of all stations between 1972 and 2006, which indicate year-to-year variability in peak discharges, are given in figure 2(a). Seasonal surface temperature anomalies indicate a tendency of higher temperatures, especially in spring and summer, in the second period (figure 2(b)). Monthly streamflow fraction (monthly streamflow over annual streamflow) and surface temperature averages from the first period (1972–88) and the changes in these variables in the second period are presented in figures 2(c) through (f). All

Table 2. Differences in annual discharges and center times, and their Monte Carlo (MC) probabilities.

	Annual runoff		Center time	
Station	Diff[a] ($m^3\ s^{-1}$)	MC prob.	Diff[a] (days)	MC prob.
Palu	8.46	0.63	4.8	0.97
Cayagzi	1.14	0.64	5.8	0.98
Karakopru	0.49	0.56	6.8	0.98
Tutak	1.63	0.64	3.5	0.92
Melekbahce	−0.53	0.46	1.9	0.79
Baykan	0.76	0.62	3.1	0.80
Bagistas	−6.86	0.24	3.5	0.91
Uzumcu	2.03	0.60	6.8	0.99

[a] Difference between the second period (1990–2006) and the first period (1972–88).

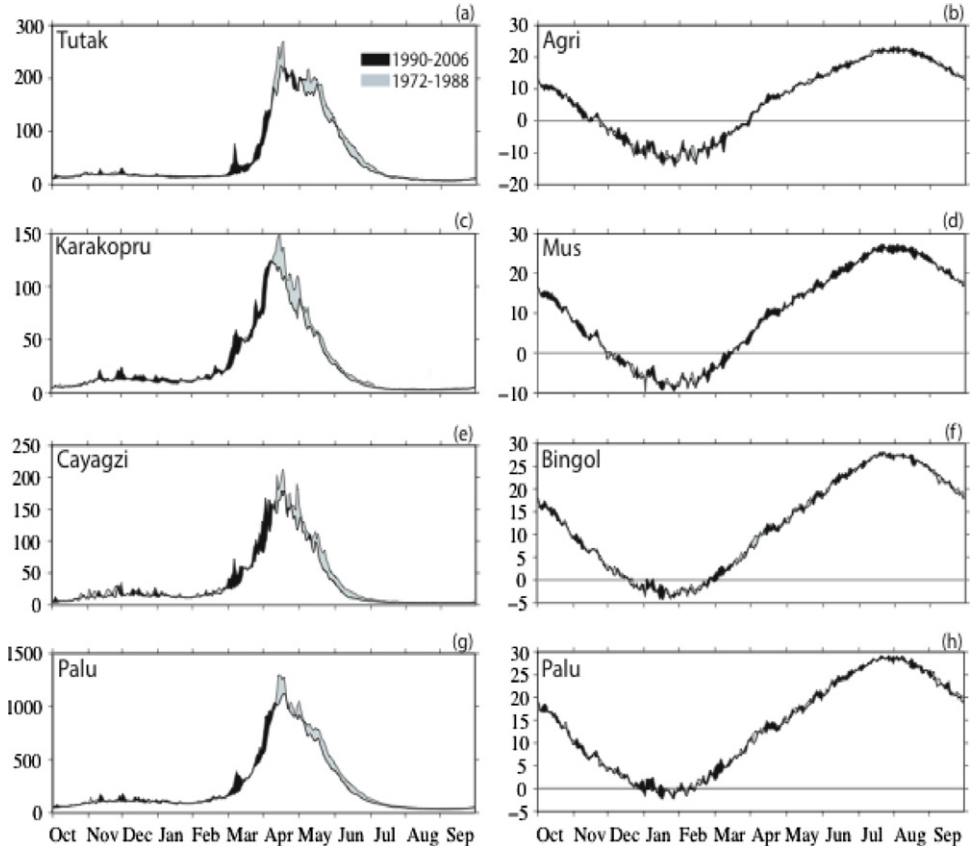

Figure 3. Daily average discharges ($m^3\ s^{-1}$) (left column) and surface temperatures (°C) (right column) from two periods (black shading indicates the excess daily discharge or surface temperature in the second period and the gray shading indicates the excess daily discharge or surface temperature in the first period): (a) for Tutak, (b) for Agri, (c) for Karakopru, (d) for Mus, (e) for Cayagzi, (f) for Bingol, (g) for Palu, and (h) for Palu.

the rivers show the typical snow-fed river characteristics (figure 2(c)). The monthly fractions of the river discharges indicate that significant melting starts in March, and ends in June and July. The majority of the peaks occur in April with 20–40% of the annual discharge. The peaks of the Uzumcu and Bagistas, however, take place in May. The difference plot (figure 2(d)) shows increases mostly occurring in March while decreases mostly happening in May, balancing each other. Monthly average surface temperatures (figure 2(e)) are usually near or below 0 °C at all meteorological stations in December, January, and February. March seems to be the transition month from below-zero to above-zero surface temperatures in the region. The monthly differences between the surface temperatures of the two periods indicate consistent warming in almost all months (figure 2(f)). There are substantial increases in winter surface temperatures (up to 1.7 °C), but they are probably not adequate to raise the surface temperatures over zero in large areas in the region. On the other hand, the increases in March (ranging from 0.5 to 1.7 °C) seem to be adequate to expose large lower-elevation areas in the basins to positive surface temperatures.

The differences in daily discharges and surface temperatures between the two periods for four station pairs are given in figure 3. The stream gauging stations are the Palu and those of its three sub-basins, and the temperature stations are the nearest ones to the gauging stations. It is clear from these plots that the discharge of the second period increases in the rising limb while it decreases in the recession limb of the major spring pulse (figures 3(a), (c), (e) and (g)). The pulse-type increase in the discharges during the first half of March in the second period is intriguing. Similar pulses appear in the other four stations as well (not shown). The pulses are followed by a brief little- or no-change period and a relatively longer increased discharge period, which usually lasts until the second week of April. These phases are especially well depicted in the Palu hydrographs (figure 3(g)). The daily surface temperature observations from the nearby climate stations indicate mostly increases in the second period (figures 3(b), (d), (f) and (h)). One of the most noticeable periods of increase takes place in late February and early March, which seems to correspond well with the timing of the remarkable early pulse in the discharge. The daily surface temperature increases during this period could be as high as about 5.5 °C in Agri, 3.5 °C in Mus, 2 °C in Bingol, and 3 °C in Palu. The other stations (Tunceli and Bitlis) also show noticeable increases in surface temperatures in this period (not shown).

In order to investigate the causes of such substantial increases in surface temperatures, we compare the average large-scale atmospheric fields obtained from the NCEP/NCAR reanalysis data for both periods (figure 4). We look into the

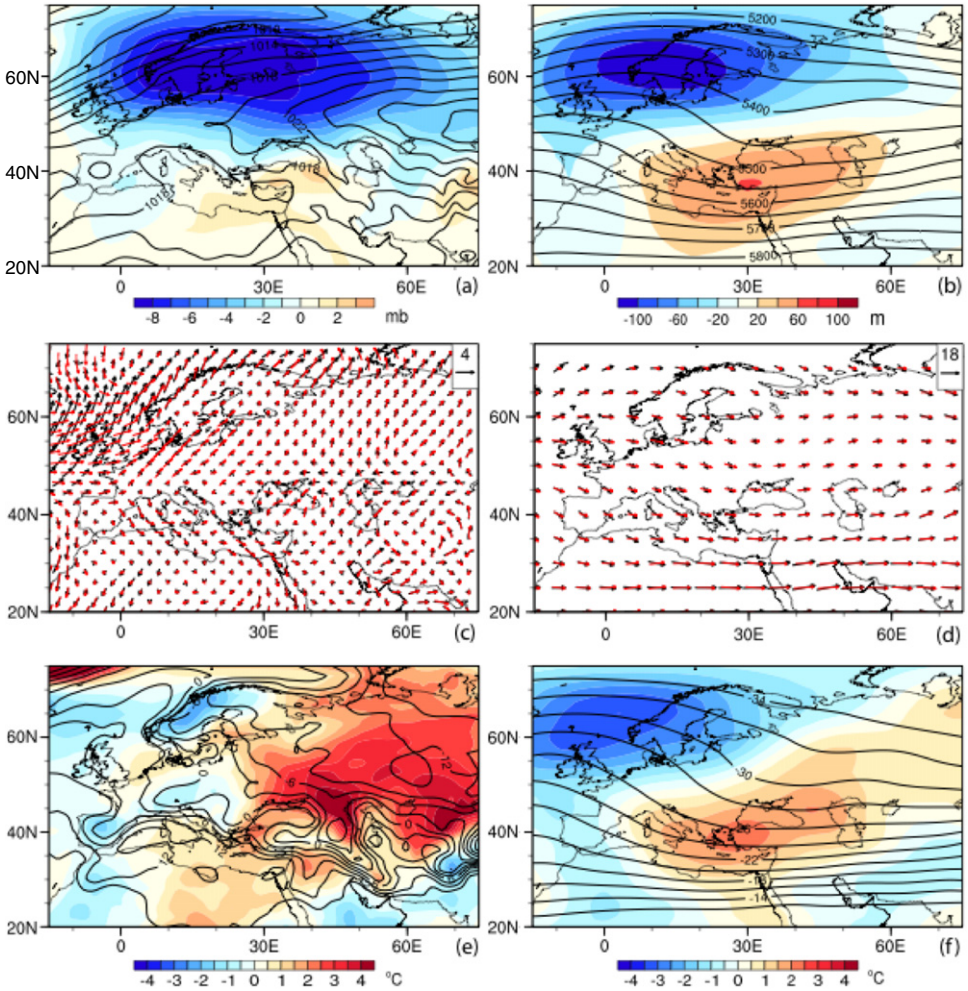

Figure 4. Average (25 February–5 March) large-scale surface and atmospheric fields calculated for the first period (1972–88) (contours or wind vectors in black) and the changes (i.e. (1990–2006) minus (1972–88)) (shaded) or the wind vectors (in red) in the second period: (a) sea level pressure (hPa), (b) 500 hPa level geopotential height (m), (c) surface wind vectors (m s^{-1}), (d) 500 hPa wind vectors (m s^{-1}), (e) surface temperature (°C), and (f) 500 hPa level temperature (°C).

time period between 25 February and 5 March. During this time of the year, the Siberian High extends toward Europe causing easterly and northeasterly surface winds over the areas between the Caspian and Black Seas, the Black Sea, the Aegean Sea and the western and northeastern parts of the Anatolian Peninsula (figures 4(a) and (c)). Typically, the easterly and northeasterly winds carry cold and dry air over these areas (Bozkurt and Sen 2011). In the second period (i.e. 1990–2006), the Siberian High weakens over Europe (the largest negative pressure anomaly is centered over the Baltic Sea), and the sea level pressures over the Anatolian Peninsula increase slightly. The surface winds start to blow from the western to southern directions (i.e. westerly, southwesterly, and southerly winds) over the aforementioned areas in response to the changes in the sea level pressures. At 500 hPa level, the negative height anomaly over the Scandinavian Peninsula and positive height anomaly over the eastern Mediterranean–Black Sea region weaken the ridge–trough pattern and result in more westerly flow over Europe and the Mediterranean Sea in the second period (figures 4(b) and (d)). Because of its relatively high elevation, eastern Anatolia is subject to negative or near-zero surface temperatures between 25 February and 5 March (figure 4(e)). In the second period, the surface temperatures increase (up to 2 °C) over this region. The surface temperatures increase over a large area including eastern Europe and northwestern Asia. The highest increase (over 4 °C) takes place over the area between the Black and Caspian Seas. The temperature change at the 500 hPa level reveals a consistent pattern with the geopotential height changes, indicating cooling over a region centered at the Norwegian Sea and warming over a region elongated from the Mediterranean Sea to the northwestern Asia (figure 4(f)). The largest warming (over 2 °C), however, occurs over the Aegean Sea and western Turkey. A time–longitude diagram of 850 hPa temperature differences (i.e. the second period minus the first period) clearly illustrates the propagation of warmer air from over the Balkans and Aegean Sea toward eastern Anatolia after about 25 February (figure 5). The largest warming in the region occurs on the first three days of March.

It is recognized that the teleconnections may help identify changes in the circulations and the climate characteristics of certain regions in the world. For this reason, we analyzed the

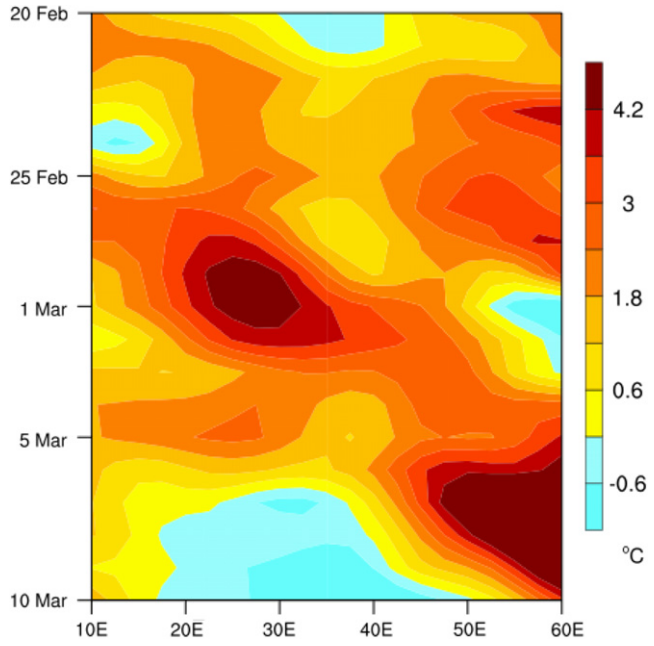

Figure 5. Time–longitude diagram of 850 hPa level temperature difference (°C) between two periods (i.e. (1990–2006) minus (1972–88)) along the latitude 39°N, which passes through the headwaters area of the Euphrates between approximately 40 and 42°E.

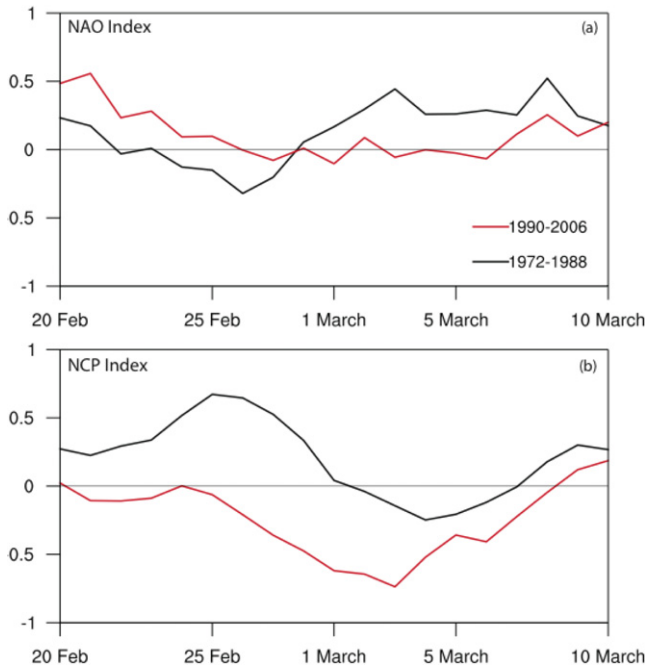

Figure 6. Daily values of the North Atlantic oscillation index (a) and North Sea–Caspian pattern index (b).

daily values of the North Atlantic oscillation (NAO) and the North Sea–Caspian pattern (NCP) indices, which are known to influence the climate of Europe and the Mediterranean basin (e.g. Hurrel 1995, Kutiel and Benaroch 2002). When the NAO index is positive (i.e. low-pressure anomalies over the Icelandic region and high-pressure anomalies over the subtropical Atlantic), the conditions are wetter and warmer than average over northern Europe and drier and colder than average over the Mediterranean regions (Visbech *et al* 2001). Cullen and deMenocal (2000) report that winter temperature and precipitation records in Turkey will reflect a cooler and drier climate during a positive phase of the NAO. In the present study, we estimated the daily NAO index using daily sea level pressure (SLP) from the NCEP/NCAR reanalysis data. The daily SLP differences obtained using the nearest grid points to Ponta Delgada (37.8°N, 25.7°W) in the Azores and Reykjavik (64.1°N, 21.9°W) in Iceland are standardized using the 1948–2010 climatological daily mean and standard deviation. The NAO index tends to have positive or near-zero values for both periods (figure 6(a)). There is not, however, any marked difference between the NAO index values of the first and second periods that can help explain the changes in the hydroclimate of eastern Anatolia in early March. Consistent with this, the use of the daily NAO index data based on the 500 hPa height anomalies (available on the web site http://www.cgd.ucar.edu/cas/jhurrell/indices.html) did not yield any remarkable difference between two periods either (not shown).

In general, the positive NCP index implies northeasterly flow toward the Balkans and the western parts of the Anatolian Peninsula, resulting in cooler temperatures, while the negative NCP index implies increased southwesterly anomaly circulation toward these areas, resulting in above normal temperatures (Kutiel and Benaroch 2002). Kutiel *et al* (2002) identifies the continental Anatolian Plateau as the region where the NCP has the maximum impact on surface temperatures. More recently, Türkes and Erlat (2009) suggest that extreme phases of the NCP index are more capable than those of the NAO index for explaining the variability in average winter temperatures in Turkey. In the present study, we estimated the daily NCP index values as described in Kutiel and Benaroch (2002) using the NCEP/NCAR reanalysis data. We calculated the differences in the average 500 hPa geopotential heights for the boxes of (0°, 55°N; 10°E, 55°N) and (50°E, 45°N; 60°E, 45°N), and then standardized them using the 1948–2010 climatological daily mean and standard deviation. The NCP index is mostly positive in the first period while it is mostly negative in the second period (figure 6(b)). There are important differences between the index values of both periods. The difference is especially remarkable from 25 February to 4 March. As suggested by Kutiel and Benaroch (2002), the negative NCP index values imply enhanced southwesterly anomaly circulation toward the Anatolian Peninsula resulting in higher surface temperatures there. The changes in the circulation and surface temperature patterns illustrated in figure 4 are also consistent with what the changes in the NCP index imply. Thus, it could be said that the early-March changes in the hydroclimate of eastern Anatolia are likely associated with the changes in the NCP.

4. Conclusions and discussion

The streamflow timings of the Euphrates and Tigris rivers are shown to be shifting to earlier days in the water year.

Six out of eight stations investigated in this study indicate statistically significant shifts ranging from 3.5 to 6.8 days between the compared two consecutive 17-year periods. It is important to mention that the changes in the timing of the streamflow occur despite no significant changes being detected in the annual streamflows. The monthly discharge differences between two periods illustrate increases mostly in March and decreases mostly in May in the second period, a zigzag-type behavior implying that the change in the streamflow timing is mainly a result of warming in the second period. Surface temperature measurements from the nearby climate stations indicate a warming signal in most of the months including March as well.

A comparison of the average daily discharges of two periods shows that the discharge of the second period increases in the rising limb while it decreases in the recession limb of the major spring pulse. The most striking increase takes place during the first half of March, and it is observed at all stream gauging sites considered in this study. The surface temperature observations at the nearby climate stations indicate substantial increases during about the same period. The reason behind this intriguing event was investigated by analyzing the NCEP/NCAR reanalysis data and atmospheric teleconnections for the period between 25 February and 5 March. In the first period (i.e. 1972–88), the Siberian High is strong over eastern Europe causing easterly, northeasterly, and northerly winds to blow over the Black Sea, northern and western parts of Turkey, and the Aegean Sea. These surface winds carry colder air from the northeast toward the southwest. In the second period, it turns out that the Siberian High is relatively weak over eastern Europe. The westerly, southwesterly, and southerly surface winds carry warmer air from southwest toward northeast. The westerly flow at the 850 hPa level helps carry the warmer air from over the central and eastern Mediterranean, Balkans, and western Anatolia to over eastern Anatolia, the Black Sea, Caspian Sea, and the land between these seas. The changes in the circulation features from the first to second periods are highly consistent with the positive and negative phases of the North Sea–Caspian pattern (NCP) identified by Kutiel and Benaroch (2002). The NCP index tends to have negative values (negative phase) for the days after 25 February in the second period. This implies enhanced southwesterly anomaly circulation toward the Anatolian Peninsula and increased surface temperatures there (Kutiel and Benaroch 2002, Kutiel *et al* 2002). Therefore, a mostly negative NCP index could be the reason behind the remarkable increase in the early-March snowmelt discharges in eastern Anatolia in the second period. The North Atlantic oscillation index is, on the other hand, found to have mostly positive or near-zero values for both periods. It does not show a noteworthy difference between two periods, therefore, it most likely has little or no effect on the changes.

Why the Siberian High weakens over eastern Europe in the second period at this time of the year is an intriguing question. Dery and Brown (2007) studied the trends of the snow cover extent in Eurasia over the period 1972–2006, presenting statistically significant negative trends in March as well as from late April to June. They also point out the larger snow-albedo feedback potential of Eurasia compared to North America. Fletcher *et al* (2009) show, albeit using model outputs, that large-scale changes in the atmospheric circulations could be caused by the snow-albedo feedback. Some studies (e.g. Stewart *et al* 2005) attribute the recent declines in snow cover extent partly to warming in the Northern Hemisphere. Given this, it may be argued that the warming in the Northern Hemisphere melts the snowpack earlier at the snow-margin areas of eastern Europe, and the excess heat as a result of the reduced albedo warms the overlying atmosphere and weakens the Siberian High by inducing vertical uplift. This theory certainly needs further research.

Temperature increases, whether they are due to climate change and/or teleconnections, may have significant implications on the water resources of eastern Anatolia. With the diminishing role of the regional snowpack as a 'natural reservoir', the importance of human-built reservoirs on the Euphrates and Tigris rivers will increase to save more water for dry spring and summer months. Furthermore, the management of several dams and hydroelectric power plants on the Euphrates and Tigris rivers will become critical to regulate the temporal distribution of water available for domestic use and irrigation to southeastern Anatolia and to downstream countries such as Iraq and Syria. Under such circumstances, it will also be challenging to sustain the precious ecosystems along both rivers.

Acknowledgment

This study is partly supported by a grant (109Y287) from TUBITAK (The Scientific and Technological Research Council of Turkey).

References

Barnett T P, Adam J C and Lettenmaier D P 2005 Potential impacts of a warming climate on water availability in snow-dominated regions *Nature* **438** 303–9

Bozkurt D and Sen O L 2011 Precipitation in the Anatolian Peninsula: sensitivity to increased SSTs in the surrounding seas *Clim. Dyn.* **36** 711–26

Cayan D R, Kammerdiener S, Dettinger M D, Caprio J M and Peterson D H 2001 Changes in the onset of spring in the western United States *Bull. Am. Meteorol. Soc.* **82** 399–415

Cullen H M and deMenocal P B 2000 North Atlantic influence on Tigris–Euphrates streamflow *Int. J. Climatol.* **20** 853–63

Daoudy M 2004 Syria and Turkey in water diplomacy (1962–2003) *Water in the Middle East and North Africa: Resources, Protection and Management* ed F Zereini and W Jaeschke (Heidelberg: Springer) pp 319–32

Dery S J and Brown R D 2007 Recent Northern Hemisphere snow cover extent trends and implications for the snow-albedo feedback *Geophys. Res. Lett.* **34** L22504

Ezber Y, Sen O L, Kindap T and Karaca M 2007 Climatic effects of urbanization in Istanbul: a statistical and modeling analysis *Int. J. Climatol.* **27** 667–79

Fletcher C G, Kushner P J, Hall A and Qu X 2009 Circulation responses to snow albedo feedback in climate change *Geophys. Res. Lett.* **36** L09702

Hamlet A F, Mote P W, Clark P M and Lettenmaier D P 2007 Twentieth-century trends in runoff, evapotranspiration, and soil moisture in the western United States *J. Clim.* **20** 1468–86

Hodgkins G A, Dudley R W and Huntington T G 2003 Changes in the timing of high river flows in New England over the 20th Century *J. Hydrol.* **278** 244–52

Hurrel J W 1995 Decadal trends in the North Atlantic oscillation: regional temperatures and precipitation *Science* **269** 676–9

IPCC 2007 *Climate Change 2007: Synthesis Report. Contribution of Working Groups I, II and III to the Fourth Assessment Report of the Intergovernmental Panel on Climate Change* ed R K Pachauri and A Reisinger (Geneva: IPCC) p 104

Kalnay E *et al* 1996 The NCEP/NCAR 40-year reanalysis project *Bull. Am. Meteorol. Soc.* **77** 437–71

Kundzewicz Z W, Mata L J, Arnell N W, Döll P, Kabat P, Jiménez B, Miller K A, Oki T, Sen Z and Shiklomanov I A 2007 Freshwater resources and their management *Climate Change 2007: Impacts, Adaptation and Vulnerability Contribution of Working Group II to the Fourth Assessment Report of the Intergovernmental Panel on Climate Change* ed M L Parry, O F Canziani, J P Palutikof, P J van der Linden and C E Hanson (Cambridge: Cambridge University Press) pp 173–210

Kutiel H and Benaroch Y 2002 North Sea–Caspian pattern (NCP)—an upper level atmospheric teleconnection affecting the Eastern Mediterranean: identification and definition *Theor. Appl. Climatol.* **71** 17–28

Kutiel H, Maheras P, Türkes M and Paz S 2002 North Sea–Caspian pattern (NCP)—an upper level atmospheric teleconnection affecting the Eastern Mediterranean—implications on the regional climate *Theor. Appl. Climatol.* **72** 173–92

McCabe G J and Clark M P 2005 Trends and variability in snowmelt runoff in the western United States *J. Hydromet.* **6** 476–82

Milly P C D, Dunne K A and Vecchia A V 2005 Global pattern of trends in streamflow and water availability in a changing climate *Nature* **438** 347–50

Moore J N, Harper J T and Greenwood M C 2007 Significance of trends toward earlier snowmelt runoff, Columbia and Missouri basin headwaters, western United States *Geophys. Res. Lett.* **34** L16402

Payne J T, Wood A W, Hamlet A F, Palmer R N and Lettenmaier D P 2004 Mitigating the effects of climate change on the water resources of the Columbia river basin *Clim. Change* **62** 233–256

Stewart I T 2009 Changes in snowpack and snowmelt runoff for key mountain regions *Hydrol. Process.* **23** 78–94

Stewart I T, Cayan D R and Dettinger M D 2005 Changes toward earlier streamflow yiming across western North America *J. Clim.* **18** 1136–55

Türkes M and Erlat E 2009 Winter mean temperature variability in Turkey associated with the North Atlantic oscillation *Meteorol. Atmos. Phys.* **105** 211–25

USCB 2009 United States Census Bureau, International Data Base (available at http://www.census.gov/ipc/www/idb/region.php, accessed 5 August 2009)

SAPRDA 2009 Southeastern Anatolian Project Regional Development Administration (available at http://www.gap.gov.tr/gap_en.php, accessed 5 August 2009)

Vincent C, Le Meur E, Six D, Funk M, Hoelzle M and Preunkert S 2007 Very high-elevation Mont Blanc glaciated areas not affected by the 20th century climate change *J. Geophy. Res.* **112** D09120

Visbech M H, Hurrell J W, Polvani L and Cullen H M 2001 The North Atlantic oscillation: past, present, and future *Proc. Natl Acad. Sci.* **98** 12876–7

Yang D, Zhao Y, Armstrong R, Robinson D and Brodzik M-J 2007 Streamflow response to seasonal snow cover mass changes over large Siberian watersheds *J. Geophy. Res.* **112** F02S22

Zhao H and Moore G W K 2006 Reduction in Himalayan snow accumulation and weakening of the trade winds over the Pacific since the 1840s *Geophys. Res. Lett.* **33** L17709